

# Functionalized Silica Nanoparticles Mitigate Salt Stress in Soybean: Comprehensive Insights of Physiological, Metabolomic, and Microbiome Responses

Zhidi Chen,<sup>▽</sup> Pan Wang,<sup>▽</sup> Simin Zhao, Yangping Sun, Yidan Liu, Sanfeng Chen, Wenfeng Chen, Gangyong Zhao, Gehong Wei,<sup>\*</sup> and Chun Chen<sup>\*</sup>



Cite This: *J. Agric. Food Chem.* 2025, 73, 10814–10825



Read Online

ACCESS |



Metrics & More



Article Recommendations



Supporting Information

**ABSTRACT:** Silica nanoparticles (SiO<sub>2</sub> NPs) have potential for mitigating salt stress in crops; however, the effects of surface modifications in enhancing their effectiveness remain unclear. This study investigated the effects of pristine and functionalized SiO<sub>2</sub> NPs (SiO<sub>2</sub>-NH<sub>2</sub> and SiO<sub>2</sub>-COOH) on soybean growth, root metabolism, and microbiome dynamics under 200 mM NaCl stress. All SiO<sub>2</sub> NPs treatments significantly reduced Na<sup>+</sup>/K<sup>+</sup>, with SiO<sub>2</sub>-COOH NPs showing the greatest efficacy, reducing by 46.6%. Enhanced salt tolerance correlated with altered root metabolism, including increased *L*-tyrosine, uridine, and indole-3-acetamide levels and enrichment of stress-response pathways. Furthermore, SiO<sub>2</sub>-COOH NPs enhanced microbial diversity, increasing the abundance of beneficial genera *Variovorax* and *Pseudomonas* in the endosphere, and *Haliangium* and *Arthrobacter* in the rhizosphere. Microbe-metabolite correlations suggest that altered root exudation under functionalized SiO<sub>2</sub> NPs treatments selectively recruits beneficial bacteria, enhancing salt tolerance. These findings highlight the potential of functionalized SiO<sub>2</sub> NPs, particularly SiO<sub>2</sub>-COOH, as nanoenabled biostimulants for sustainable agriculture.

**KEYWORDS:** silica nanoparticles, surface modification, Na<sup>+</sup>/K<sup>+</sup>, root exudates, rhizobacteria

## INTRODUCTION

Soil salinity poses a significant threat to global food security by severely impairing crop growth and productivity.<sup>1</sup> This widespread problem arises from the accumulation of sodium (Na<sup>+</sup>) and chloride (Cl<sup>-</sup>) ions in the soil, leading to hyperosmotic conditions that disrupt plant water and nutrient uptake.<sup>2</sup> Excessive Na<sup>+</sup> disrupts ion homeostasis within plant cells, which hinders the absorption of essential nutrients like K<sup>+</sup>, Ca<sup>2+</sup>, Mg<sup>2+</sup>, and Zn<sup>2+</sup>, ultimately compromising key physiological processes such as photosynthesis and metabolism.<sup>3,4</sup> Soybean (*Glycine max* L.) is a globally important legume crop and a significant source of protein and oil for human and animal consumption.<sup>5</sup> However, soybean is particularly susceptible to salt stress, especially during the seedling stage.<sup>6</sup> Excessive Na<sup>+</sup> accumulation in soybean tissues can lead to oxidative damage, disrupting membrane systems, degrading proteins, and impairing photosynthetic capacity, ultimately resulting in reduced yield and quality.<sup>7,8</sup> Soil salinization poses a significant challenge to soybean production, and developing effective strategies to enhance soybean salt tolerance is, therefore, essential for safeguarding food security and meeting the growing demand for this valuable crop.

Silicon (Si) has emerged as a beneficial element that can alleviate various abiotic stresses in plants.<sup>9</sup> Traditional Si amendments, such as silicate fertilizers, have shown some success in mitigating salt stress by promoting root development and reducing the adverse effects of NaCl accumulation.<sup>10</sup> However, their effectiveness of these conventional methods is

often limited by poor Si bioavailability and inefficient plant uptake.<sup>11</sup> Recent advances in nanotechnology present a promising alternative, offering a more sustainable approach to enhancing plant Si nutrition and stress tolerance.

Silica nanoparticles (SiO<sub>2</sub> NPs) have shown considerable potential in enhancing plant salt tolerance. Compared to conventional agrichemicals, SiO<sub>2</sub> NPs exhibit unique physicochemical properties, such as high surface area and reactivity, which improve the delivery and uptake of Si in plant tissues.<sup>12</sup> Studies have demonstrated that SiO<sub>2</sub> NPs can notably alleviate salt stress by reducing Na<sup>+</sup> accumulation, improving K<sup>+</sup>/Na<sup>+</sup> ratio;<sup>13</sup> enhancing nutrient uptake;<sup>14</sup> increasing osmolyte production like proline;<sup>7</sup> and strengthening antioxidant defenses.<sup>15</sup> Although these results are promising, there is still potential to make pristine SiO<sub>2</sub> NPs even more effective.

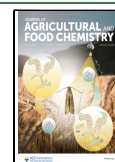
Functionalizing SiO<sub>2</sub> NPs with specific chemical groups provides an opportunity to optimize their interactions with plants and the surrounding soil environment, potentially improving their uptake, targeting specific cellular compartments, and modulating their biological activity.<sup>16</sup> The choice of functional groups is crucial for determining the effectiveness of nanoparticles in biological systems. In this study, we selected

**Received:** January 5, 2025

**Revised:** April 15, 2025

**Accepted:** April 15, 2025

**Published:** April 24, 2025



amino ( $-\text{NH}_2$ ) and carboxyl ( $-\text{COOH}$ ) groups for functionalization based on two considerations. First, both amino and carboxyl groups can increase the hydrophilicity and dispersibility of  $\text{SiO}_2$  NPs in aqueous solutions,<sup>17</sup> which is crucial for their uptake and translocation in plants. Second, these functional groups can introduce positive ( $\text{NH}_2$ ) or negative ( $\text{COOH}$ ) charges on the nanoparticle surface, potentially influencing their interactions with negatively charged cell walls and membranes of plant cells,<sup>18</sup> as well as with charged soil components. Various functional groups, including APTES (3-aminopropyltriethoxysilane) and amino acids, have been explored to enhance the efficiency<sup>19,20</sup> and biocompatibility of  $\text{SiO}_2$  NPs under stress conditions.<sup>21</sup> These modifications can reduce the surface polarity of  $\text{SiO}_2$  NPs, potentially altering their interactions with plant cells and soil components. Despite these advancements, the potential of functionalized  $\text{SiO}_2$  NPs for enhancing plant salt tolerance has not been fully explored.

In addition to their direct effects on plants,  $\text{SiO}_2$  NPs may influence the plant-associated microbiota, which plays a crucial role in plant health and productivity.<sup>22</sup> The rhizosphere and root endosphere host diverse microbiota that interact symbiotically with plants, aiding in nutrient absorption, pathogen resistance, and environmental adaptation.<sup>23,24</sup> These microbial communities are particularly important in assisting plants to cope with salt stress.<sup>25,26</sup> For instance, inoculating the soybean rhizosphere with beneficial bacteria like *Pseudomonas pseudoalcaligenes* and *Bacillus subtilis* has been shown to enhance salt tolerance.<sup>27</sup>  $\text{SiO}_2$  NPs have also been reported to stimulate the growth of plant growth-promoting rhizobacteria (PGPR) and increase the total soil bacterial population in the soil, suggesting their potential as effective tools for enhancing PGPR activity in the rhizosphere.<sup>28</sup> Moreover, short-term application of silicate fertilizer in rice cropping systems has been shown to markedly altered the soil microbiome, enhancing functions related to labile carbon degradation, carbon and nitrogen fixation, and phosphorus acquisition.<sup>29</sup> However, studies on the response of root-associated microbes to pristine and functionalized  $\text{SiO}_2$  NPs application, particularly under stress conditions, remain limited.

This study addresses this gap by investigating the effects of pristine and functionalized  $\text{SiO}_2$  NPs ( $\text{SiO}_2\text{-NH}_2$  and  $\text{SiO}_2\text{-COOH}$  NPs) on soybean salt tolerance. We hypothesize that functionalized  $\text{SiO}_2$  NPs, with their altered surface properties, will be more effective in mitigating salt stress in soybean compared to pristine  $\text{SiO}_2$  NPs. Specifically, we propose that these surface modifications enhance the nanoparticles' ability to (1) modulate root exudate profiles, leading to the release of signaling molecules that promote beneficial plant-microbe interactions; and (2) interact selectively with soil components and rhizosphere microbes, thereby creating a more favorable microenvironment to support plant growth under salt stress conditions. To test this hypothesis, we assessed the impact of pristine and functionalized  $\text{SiO}_2$  NPs on soybean growth, the  $\text{Na}^+/\text{K}^+$  ratio, root exudate profiles, and root bacterial community structure under salt stress. This study enhances our understanding of how pristine and functionalized nanomaterials can be applied to sustainable agricultural practices.

## MATERIALS AND METHODS

**Synthesis and Characterization of  $\text{SiO}_2\text{-NH}_2$  and  $\text{SiO}_2\text{-COOH}$  NPs.** Pristine  $\text{SiO}_2$  NPs (20 nm, 99 wt %) were purchased from

XFNANO Materials Tech Co., Ltd. (Jiangsu, China). Amino-functionalized  $\text{SiO}_2$  NPs ( $\text{SiO}_2\text{-NH}_2$  NPs) were synthesized by treating pristine  $\text{SiO}_2$  NPs with 3-aminopropyltriethoxysilane (APTES) according to the method described by Hiebner et al.<sup>30</sup> Subsequently, the  $\text{SiO}_2\text{-NH}_2$  NPs were reacted with succinic anhydride to obtain carboxyl-functionalized  $\text{SiO}_2$  NPs ( $\text{SiO}_2\text{-COOH}$  NPs), following the procedure described by Rehman et al.<sup>31</sup> Additional details regarding the synthesis can be found in the Supporting Information.

**Plant Materials and Growth Conditions.** Soybean (Zhonghuang13) seeds were purchased from the Hongfeng High-tech Seed Industry (Henan, China). The soil used in this study was collected from Yangling, Shaanxi, China ( $34^\circ 12' \text{ N}$ ,  $108^\circ \text{ E}$ ). The physicochemical properties of the soil were as follows: pH (1:2.5 soil: water)  $8.32 \pm 0.03$ ; electrical conductivity (EC)  $94.25 \pm 4.9 \mu\text{S cm}^{-1}$ ; AP  $9.57 \pm 0.24 \text{ mg kg}^{-1}$ ;  $\text{NH}_4^+\text{-N}$   $1.19 \pm 0.12 \text{ mg kg}^{-1}$ ;  $\text{NO}_3^-\text{-N}$   $8.49 \pm 0.74 \text{ mg kg}^{-1}$ ; and SOM  $12.65 \pm 1.48 \text{ g kg}^{-1}$ . The final  $\text{Na}^+$  content in the soil was  $1.17 \text{ g/kg}$ . More details on seed germination and soil pretreatment can be found in the Text S2.

**Pot Experiment.** To explore the effects of functionalized  $\text{SiO}_2$  NPs on soybean growth under salt stress, five treatments were designed: (1) Control (nonsalt stress); (2) NaCl (200 mM NaCl salt stress); (3)  $\text{SiO}_2$  (pristine  $\text{SiO}_2$  NPs + salt stress); (4)  $\text{SiO}_2\text{-NH}_2$  ( $\text{SiO}_2\text{-NH}_2$  NPs + salt stress); (5)  $\text{SiO}_2\text{-COOH}$  ( $\text{SiO}_2\text{-COOH}$  NPs + salt stress). For the NPs treatments, pristine  $\text{SiO}_2$  NPs,  $\text{SiO}_2\text{-NH}_2$  NPs, and  $\text{SiO}_2\text{-COOH}$  NPs were added to the soil at a final silicon application rate of 1 g of  $\text{SiO}_2/\text{kg}$  of dry soil. Each treatment with six replicates. Six uniformly grown soybean seedlings were selected and transplanted into pots. After 1 week, the seedlings were thinned to three plants per pot. The pots were maintained at 60% of the field capacity in an artificial climate chamber (College of Life Science, Northwest A&F University, China) at  $25^\circ\text{C}/20^\circ\text{C}$  (day/night) and the relative humidity was maintained at 50–60% with a 14 h photoperiod. Regular irrigation with deionized water was carried out every 5 days, and soybeans were harvested after 1 month of growth.

**Determination of Soybean Growth and Physiological Properties.** After 30 days of cultivation (R4 growth stage), the photosynthetic rate, stomatal conductance, and transpiration rate of soybeans were measured under adequate light using a portable photosynthesis system (LI-6400xt, LI-COR Inc., Lincoln, NE).<sup>32</sup> The value of SPAD (Soil and Plant Analyzer Development) was determined by SPAD-502 (Spectrum Technologies, Plainfield, IL). The fresh weights of the shoots and roots were recorded separately. Root traits, including total root length and number of root tips, were analyzed using root scanning (WinRHIZO, Regent, Canada). Afterward, the root systems of each plant were dried to a constant weight. Dried samples were ground for ion analysis. The concentrations of  $\text{Na}^+$  and  $\text{K}^+$  were measured by a flame photometer (ZA3000, Hitachi, Japan),<sup>33</sup> and Si content was measured using inductively coupled plasma mass spectrometry (ICP-MS) (Agilent 7900).<sup>34</sup>

**Determination of Soil Physical and Chemical Properties.** Soil available potassium (AK) was determined by flame photometry after extraction with ammonium acetate solution.<sup>35</sup> AP was determined with the Olsen method.<sup>36</sup>  $\text{NH}_4^+\text{-N}$  and  $\text{NO}_3^-\text{-N}$  were extracted using 1 M potassium chloride (KCl) and measured using an AA3 Continuous Flow Analyzer (Skalar SAN, SKALAR, Breda).<sup>35</sup> The SOM content was analyzed using a TOC-HT1300 total organic carbon analyzer (Analytikjena, Germany), following the method described by Yu et al.<sup>37</sup>

**Collection of Root Exudates and Metabolomic Analysis.** Roots were cleaned using sterile water and transferred to plastic containers with 100 mL of dd  $\text{H}_2\text{O}$ .<sup>38</sup> After 24 h, the culture media were filtered through 0.22  $\mu\text{m}$  filter membranes and freeze-dried. All samples were stored at  $-80^\circ\text{C}$  until analysis. Metabolomic analysis was conducted on six biological replicates for each treatment. Root exudate components were determined by liquid chromatography–mass spectrometry (LC-MS). Further details on sample analysis by LC-MS and data processing can be found in the Text S3.

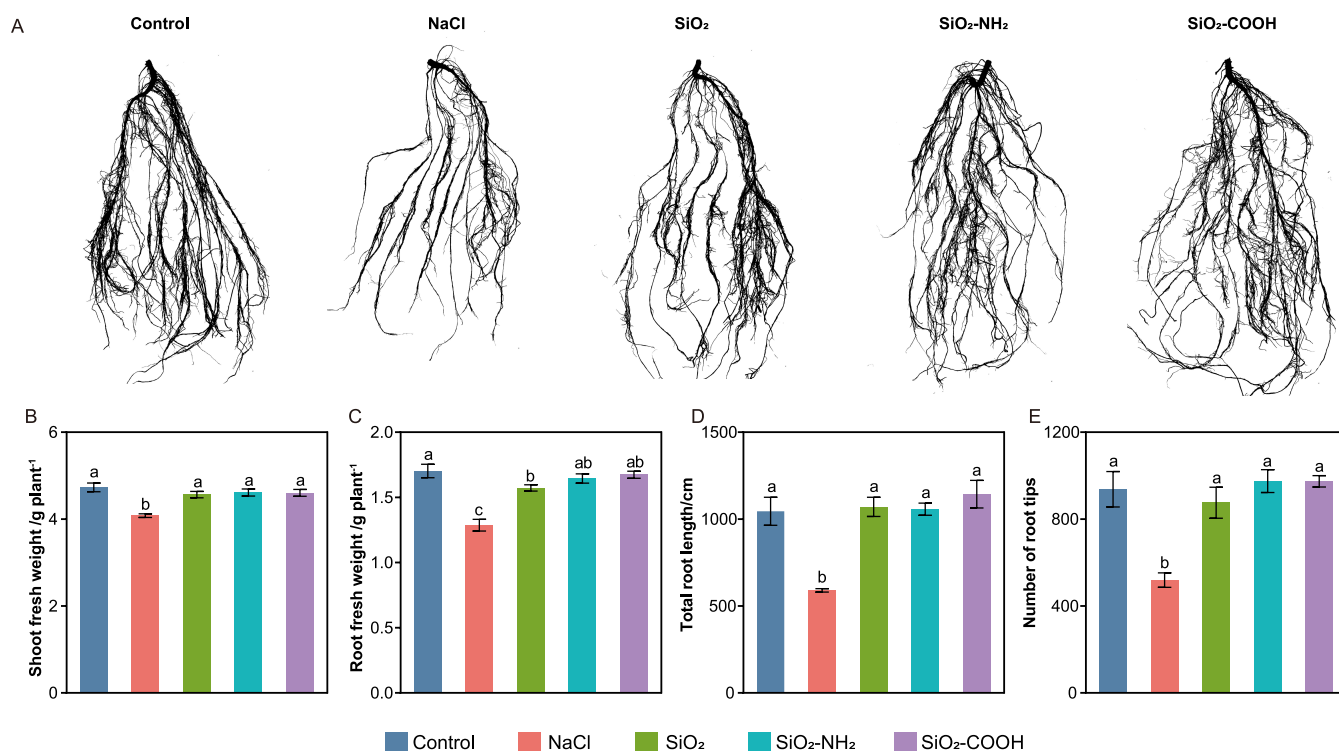


**Figure 1.** Scanning photographs of root (A), shoot fresh weight (B), root fresh weight (C), total root length (D), and number of root tips (E) of soybeans under different treatments. Data are shown as mean  $\pm$  SE, with  $n = 6$ . Lowercase letters show the significant differences across treatments ( $p < 0.05$ ). Control: nonsalt stress, NaCl: salt stress, SiO<sub>2</sub>: pristine SiO<sub>2</sub> NPs + salt stress, SiO<sub>2</sub>-NH<sub>2</sub>: SiO<sub>2</sub>-NH<sub>2</sub> NPs + salt stress, SiO<sub>2</sub>-COOH: SiO<sub>2</sub>-COOH NPs + salt stress.

### 16S rRNA Amplicon Sequencing of Rhizosphere and Endophytic Bacteria.

The bacterial community composition was analyzed by high-throughput sequencing of the 16S rRNA gene.<sup>39</sup> The total DNA was extracted from 0.5 g of rhizosphere soil and 0.5 g of roots using a FastDNA SPIN Kit for Soil (MP Biomedicals). The concentration and purity of the extracted DNA were measured using a Nanodrop 2000 (Thermo Fisher Scientific, MA). The 16S rRNA genes were amplified using primer pairs 799F: 1193R (targeting the V5–V7 region of the marker gene) for roots and 515F: 926R (V4–V5) for soils.<sup>40</sup> Sequencing procedure was performed with an Illumina MiSeq platform at Guangdong Magigene Biotechnology Co., Ltd. (Guangzhou, China). Data processing details are provided in the Text S4.

**Statistical Analysis.** All figures were drawn with GraphPad Prism 9 graphical software and the “ggplot2” package in R software (version 4.3.2).<sup>41</sup> Differences between treatments were further assessed by Duncan’s multiple range test with a significance level of  $p < 0.05$ , following one-way analysis of variance (ANOVA) using SPSS 16.0 software (SPSS Inc., Chicago, IL).<sup>42</sup> Each treatment included six replicates. The  $\alpha$  diversity of the microbial communities was estimated by using the Shannon and Chao1 indices based on the observed ASVs.  $\beta$  diversity was assessed through principal coordinate analysis (PCoA) based on Bray–Curtis distance. Analysis of similarities (ANOSIM) was performed using the Adonis function in the “vegan” package in R. Prediction of the functional potential of rhizosphere and endosphere bacterial communities using PICRUSt2.<sup>43</sup> Differential abundance KEGG pathway analysis was performed using STAMP software with the proportion difference test and the Benjamini–Hochberg FDR correction. Partial least-squares discriminant analysis (PLS-DA) was performed on the preprocessed metabolomics data using MetaboAnalyst 5.0.<sup>44</sup> Differential metabolites were screened by  $VIP > 1$ ,  $p < 0.05$ , and  $|\log_2 FCI| > 1$ .<sup>45</sup> The Spearman correlation between microbial relative abundance, Na<sup>+</sup>/K<sup>+</sup> ratio, and metabolite content was calculated by “psych” package, retaining only those significant ( $p < 0.05$ ).<sup>46</sup> Correlations with  $p < 0.05$ ,  $|r| > 0.6$  were selected for network construction, and the

network was visualized using Cytoscape 3.10.1.<sup>41</sup> We identified putative keystone metabolites and ASVs based on network topology using a fast greedy algorithm to calculate within-module connectivity ( $Z_i$ ) and among-module connectivity ( $P_i$ ) for each node. Nodes with  $Z_i > 2.5$  were designated as module hubs, while nodes with  $P_i > 0.62$  were designated as connectors among different modules. Nodes with both  $Z_i > 2.5$  and  $P_i > 0.62$  were designated as network hubs.<sup>47</sup>

## RESULTS AND DISCUSSION

**Characterization of Pristine and Functionalized SiO<sub>2</sub> NPs.** We characterized three types of SiO<sub>2</sub> NPs using scanning electron microscopy (SEM), transmission electron microscopy (TEM), Fourier transform infrared spectrometry (FT-IR), and  $\zeta$ -potential measurements. The pristine SiO<sub>2</sub>, SiO<sub>2</sub>-NH<sub>2</sub>, and SiO<sub>2</sub>-COOH NPs exhibited spherical morphology with average hydrodynamic diameters of  $27.7 \pm 1.7$ ,  $47.9 \pm 1.8$ , and  $37.8 \pm 2.2$  nm, respectively (Figure S1D). The typical absorption bands at 961 and 1088 cm<sup>-1</sup> shown in Figure S1C can be assigned to the characteristic bands of Si, and the weak peak at 2900 cm<sup>-1</sup> corresponds to the stretching vibration of C–H. Compared with the spectra for pristine SiO<sub>2</sub> and SiO<sub>2</sub>-NH<sub>2</sub> NPs, a new peak at 1500–2000 cm<sup>-1</sup> in the spectra of SiO<sub>2</sub>-COOH NPs appears, which can be assigned to the C=O stretch vibration band. FT-IR analysis confirmed the successful functionalization of the SiO<sub>2</sub> NPs, with amino and carboxyl groups effectively attached to the nanoparticle surfaces (Figure S1C).  $\zeta$ -potential analysis indicated the surface charges for each type:  $-28.7 \pm 2.1$  mV for pristine SiO<sub>2</sub> NPs,  $12.2 \pm 0.9$  mV for SiO<sub>2</sub>-NH<sub>2</sub> NPs, and  $-13.6 \pm 0.6$  mV for SiO<sub>2</sub>-COOH NPs (Figure S1E). These different functional groups present on the nanoparticle surface affect the surface charge and reduce the surface polarity of SiO<sub>2</sub> NPs, which impact their interactions with plant and soil environments.<sup>48</sup>

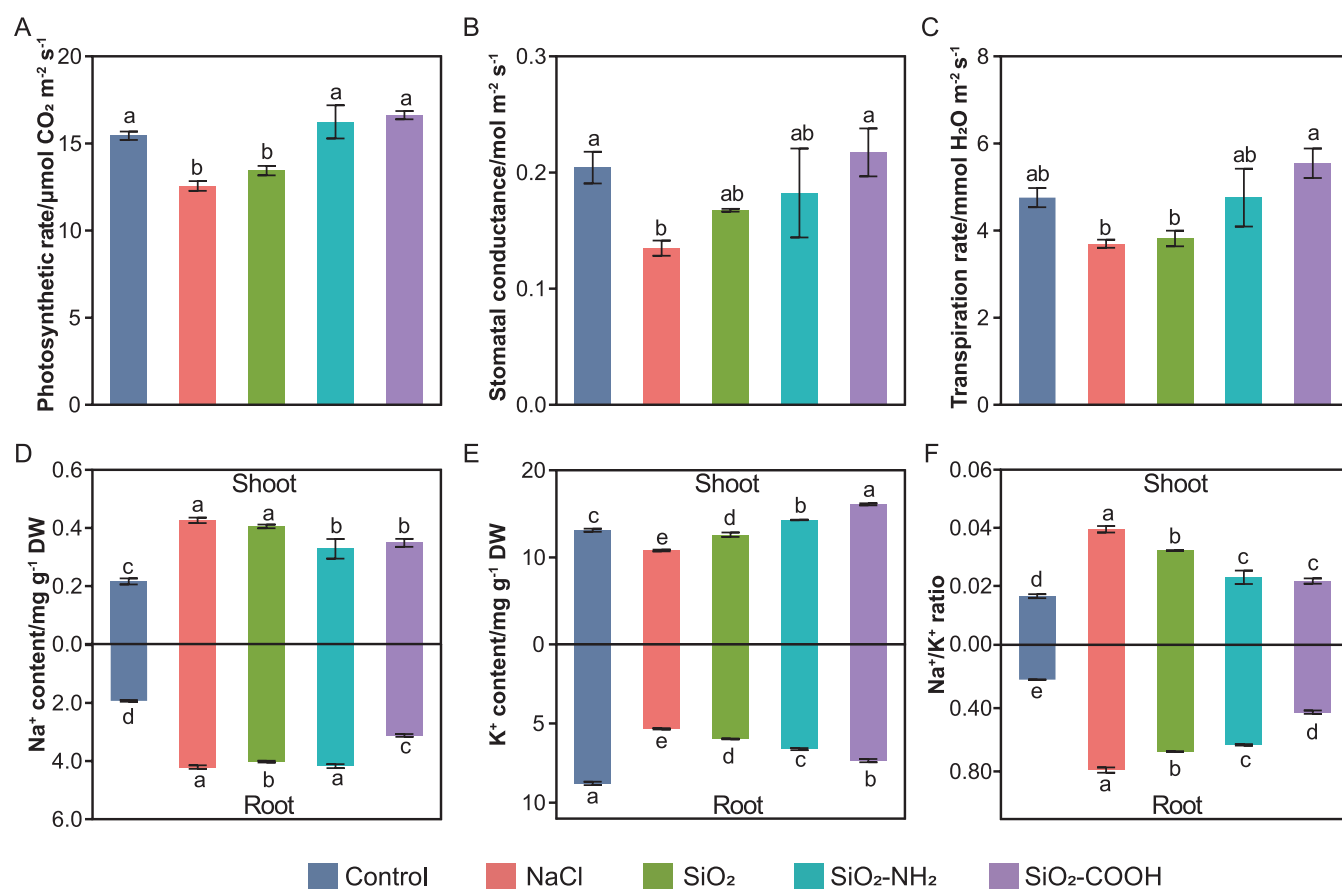


**Figure 2.** Photosynthetic rate (A), stomatal conductance (B), transpiration rate (C), Na<sup>+</sup> content (D), K<sup>+</sup> content (E), and Na<sup>+</sup>/K<sup>+</sup> ratio (F) of soybean under different treatments. Data are shown as mean  $\pm$  SE,  $n = 6$ . Letters show the significant differences across treatments ( $p < 0.05$ ). Control: nonsalt stress, NaCl: salt stress, SiO<sub>2</sub>: pristine SiO<sub>2</sub> NPs + salt stress, SiO<sub>2</sub>-NH<sub>2</sub>: SiO<sub>2</sub>-NH<sub>2</sub> NPs + salt stress, SiO<sub>2</sub>-COOH: SiO<sub>2</sub>-COOH NPs + salt stress.

**Effects of Pristine and Functionalized SiO<sub>2</sub> NPs on Soybean Growth.** To investigate the effects of SiO<sub>2</sub> NPs on soybean under salt stress, we examined changes in plant growth and root development in both salt-stressed and SiO<sub>2</sub> NPs treated plants. Compared to the nonstressed control, salt stress caused a significant reduction in plant biomass and root development, with reductions in shoot fresh weight (13.8%), root fresh weight (24.5%), total root length (43.5%), and root tip number (44.6%) (Figure 1 B–E). However, soybean plants treated with both pristine and functionalized SiO<sub>2</sub> NPs exhibited significant improvements in growth, especially in root architecture, compared to those under NaCl stress (Figure 1 A). Both pristine and functionalized SiO<sub>2</sub> NPs treatments led to significant increases in shoot fresh weight (11.9–13.1%), root fresh weight (22.3–30.1%), total root length (79.1–93.8%), and the number of root tips (68.6–87.7%) ( $p < 0.05$ , Figure 1B–E) compared with NaCl treatment. These parameters did not differ significantly from the nonsalt stress group ( $p > 0.05$ ), indicating that salt stress inhibited soybean growth and root development, but the application of SiO<sub>2</sub> NPs effectively mitigated these adverse effects.<sup>49</sup> A robust root system is crucial for efficient water and nutrient uptake, especially in saline conditions.<sup>50</sup> The observed increases in root length and number of root tips likely contribute to more effective water and nutrient absorption, thus supporting improved plant growth even in high-salinity conditions. However, no significant differences were observed between

the effects of pristine and functionalized SiO<sub>2</sub> NPs ( $p > 0.05$ ). The absence of significant differences in growth parameters between pristine and functionalized SiO<sub>2</sub> NPs may be attributed to several factors. First, the similar Si content in soybean tissues across all NPs treatments (Figure S3B,C) suggests comparable Si uptake and accumulation, which could explain the similar growth responses. Second, our experiment focused on the early growth stages of soybean (30 days postplanting). The effects of surface functionalization on growth may become more pronounced at later developmental stages under prolonged salt stress exposure.

In addition, compared with the control, salt stress significantly affected the photosynthetic parameters of plants (Figure 2 A–C). In particular, the photosynthetic rate, stomatal conductance, and transpiration rate decreasing by 18.7, 34.0, and 22.2%, respectively. In comparison to salt-stressed plants, SiO<sub>2</sub>-COOH treatment significantly enhanced the photosynthetic parameters in soybean. Specifically, the photosynthetic rate, stomatal conductance, and transpiration rate were increased by 1.32-, 1.61-, and 1.50-fold, respectively (Figure 2 A–C). Compared with NaCl, the SPAD value increased by 25.6% under SiO<sub>2</sub>-COOH NPs treatment, and a similar significant increase (19.3%) was observed under SiO<sub>2</sub>-NH<sub>2</sub> NPs treatment (Figure S3A). This is consistent with the results of Lu et al.,<sup>51</sup> who found that the chlorophyll content of *Arabidopsis thaliana* was increased under the treatment of amine-functionalized SiO<sub>2</sub> NPs. Additionally, the observed

increase in stomatal conductance (Figure 2 B) suggests that functionalized SiO<sub>2</sub> NPs may improve stomatal regulation under salt stress. By promoting stomatal opening, these NPs could enhance CO<sub>2</sub> availability for photosynthesis.<sup>52</sup> Furthermore, salt stress often leads to excessive Na<sup>+</sup> accumulation, which disrupts cellular osmotic balance, causes water deficit, and impairs photosynthetic function. By reducing Na<sup>+</sup> accumulation and maintaining K<sup>+</sup> homeostasis, functionalized SiO<sub>2</sub> NPs may alleviate osmotic stress, thereby creating a more favorable intracellular environment for photosynthesis activity.<sup>53</sup> Our findings suggest that functionalized SiO<sub>2</sub> NPs may exert comparable effects in soybeans, promoting photosynthesis under salt stress conditions.

Maintaining a balanced Na<sup>+</sup>/K<sup>+</sup> ratio is vital for plant survival under salinity stress, as it directly impacts osmotic adjustment, nutrient acquisition, and enzyme activity.<sup>54</sup> Previous studies have shown that Si application can reduce Na<sup>+</sup> uptake and translocation while increasing K<sup>+</sup> uptake under salinity stress.<sup>55</sup> Consistent with these observations, our results demonstrated that both pristine and functionalized SiO<sub>2</sub> NPs significantly reduced Na<sup>+</sup> accumulation and promoted K<sup>+</sup> uptake in soybeans, leading to a reduction in the Na<sup>+</sup>/K<sup>+</sup> ratio (Figure 2 D–F). Compared to the control, the Na<sup>+</sup>/K<sup>+</sup> ratio significantly increased in plants under salt stress with a 1.4-fold increase in shoots and a 2.6-fold increase in roots. However, both pristine and functionalized SiO<sub>2</sub> NPs significantly reduced the Na<sup>+</sup>/K<sup>+</sup> ratio, with reductions ranging from 14.8 to 46.6% in roots and from 18.0 to 44.9% in shoots, compared to NaCl. Notably, functionalized SiO<sub>2</sub> NPs, especially SiO<sub>2</sub>-COOH NPs, exhibited a more pronounced effect in lowering the Na<sup>+</sup>/K<sup>+</sup> ratio than pristine SiO<sub>2</sub> NPs, even though the Si content remained consistent across all three treatments (Figure S3B,C). This observation suggests that the enhanced efficacy of functionalized SiO<sub>2</sub> NPs is likely due to their modified surface properties. Specifically, the carboxyl groups on SiO<sub>2</sub>-COOH NPs play a crucial role in regulating ion uptake at the root-soil interface.<sup>56</sup> These functional groups can directly interact with Na<sup>+</sup> in the soil solution, effectively binding Na<sup>+</sup> and reducing its availability for plant uptake.<sup>21</sup> By reduction of Na<sup>+</sup> accumulation in plant tissues, this mechanism alleviates salt stress, thereby supporting overall plant growth and physiological performance. Furthermore, the presence of carboxyl groups on the nanoparticle surface may also influence the expression and activity of ion transporters in plant roots.<sup>57</sup>

**Metabolic Response of Soybean Roots to Exposure of Pristine and Functionalized SiO<sub>2</sub> NPs.** Root exudates, complex mixtures of organic compounds secreted by plant roots, play a crucial role in mediating plant-microbe interactions and shaping the rhizosphere environment.<sup>58</sup> Our study shows that the application of SiO<sub>2</sub> NPs can promote root development and reduce the Na<sup>+</sup>/K<sup>+</sup> ratio, which directly affects root metabolism. To explore the metabolic response of soybean exposure to pristine and functionalized SiO<sub>2</sub> NPs under salt stress. We analyzed root exudates from five treatments (control, NaCl, SiO<sub>2</sub>, SiO<sub>2</sub>-NH<sub>2</sub>, and SiO<sub>2</sub>-COOH) using a metabolomics approach based on LC-MS/MS. A total of 920 root metabolites were identified. The partial least-squares discriminant analysis (PLS-DA) of all detected metabolites revealed clear separation between the NPs treated groups and the NaCl group along the first principal component axis (Figure S4A,B). Moreover, analysis of similarities (ANOSIM) indicated that SiO<sub>2</sub> NPs significantly affected root metabolite profiles under salt stress (Table S4). We

identified and extracted differentially expressed metabolites (DEMs) across seven groups: Control vs NaCl, SiO<sub>2</sub> vs NaCl, SiO<sub>2</sub>-NH<sub>2</sub> vs NaCl, SiO<sub>2</sub>-COOH vs NaCl, SiO<sub>2</sub>-NH<sub>2</sub> vs SiO<sub>2</sub>, SiO<sub>2</sub>-COOH vs SiO<sub>2</sub>, and SiO<sub>2</sub>-COOH vs SiO<sub>2</sub>-NH<sub>2</sub>. Compared to the control, plants subjected to salt stress showed an increase in the secretion of lipids and lipid-like molecules. However, the addition of SiO<sub>2</sub> NPs reduced the secretion of these molecules and increased the secretion of organic heterocyclic compounds, as well as amino acids, peptides, and analogs (Figure S4C,D). These changes are beneficial for maintaining root osmotic pressure, thereby reducing Na<sup>+</sup> absorption and alleviating Na<sup>+</sup>/K<sup>+</sup> imbalance.<sup>7</sup>

To further understand the functional significance of these metabolic changes, KEGG pathway analysis was performed to identify the most significantly enriched pathways (Figure S5). The analysis identified significant enrichment of 6 pathways in the SiO<sub>2</sub> vs NaCl, 7 pathways in the SiO<sub>2</sub>-NH<sub>2</sub> vs NaCl, and 6 pathways in SiO<sub>2</sub>-COOH vs NaCl, primarily associated with amino acid metabolism, including arginine and proline metabolism pathways. These findings highlight the critical role of amino acid metabolism in plant responses to salt stress. Amino acids contribute to osmotic adjustment, reactive oxygen species (ROS) detoxification, and the maintenance of protein synthesis under saline conditions.<sup>59</sup> Proline, for example, mitigates the detrimental effects of osmotic stress on cell turgor and enzyme activity.<sup>60</sup> Arginine serves as a precursor for polyamine biosynthesis; these osmoprotectants contribute to preserving cellular integrity and function during stress.<sup>61</sup> Under salt stress, the secretion of amino acid metabolites in soybean roots was significantly reduced. However, all three types of SiO<sub>2</sub> NPs treatments significantly upregulated metabolites in amino acid metabolism, including L-tyrosine (26.02–60.45-fold), L-tryptophan (1.43–2.26-fold), L-phenylalanine (17.33–36.94-fold), and tryptamine (1.95–2.56-fold). Additionally, metabolites in the indole alkaloid metabolism, such as 3-indoleacetonitrile (4.93–11.48-fold), indole-3-acetamide (6.32–7.03-fold), as well as uridine (6.23–9.96-fold) in the purine metabolism, were significantly upregulated. Importantly, SiO<sub>2</sub>-NH<sub>2</sub> NPs induced the highest increase in 3-indoleacetonitrile levels compared to other treatments (Figure S6). These metabolites are essential for plant osmoregulation, accumulating as compatible solutes in plant cells to maintain cell expansion under osmotic stress.<sup>62,63</sup> Amino acids, such as L-tryptophan, serve as precursors for signaling molecules that enhance plant defense responses, potentially improving stress tolerance.<sup>64</sup> Specifically, L-tyrosine is a precursor for the biosynthesis of various secondary metabolites involved in plant stress responses, including flavonoids, lignin, and salicylic acid. Flavonoids are known to possess antioxidant properties and can scavenge ROS generated under salt stress. The increased production of L-tyrosine observed in our study may therefore contribute to enhanced salt tolerance in soybean by promoting the biosynthesis of these protective compounds.<sup>65</sup> Indole-3-acetamide, a key precursor in the indole-3-acetic acid (IAA) biosynthesis pathway, promotes root development, which is essential for maintaining water and nutrient uptake and thus, improving plant survival and growth under salt stress.<sup>66,67</sup> These findings highlight the critical role of specific metabolites in enhancing plant resilience under salt stress.

**Microbial Community Response in Endosphere and Rhizosphere to Pristine and Functionalized SiO<sub>2</sub> NPs.** High-throughput sequencing of bacterial 16S rRNA genes was performed to assess the responses of endosphere and

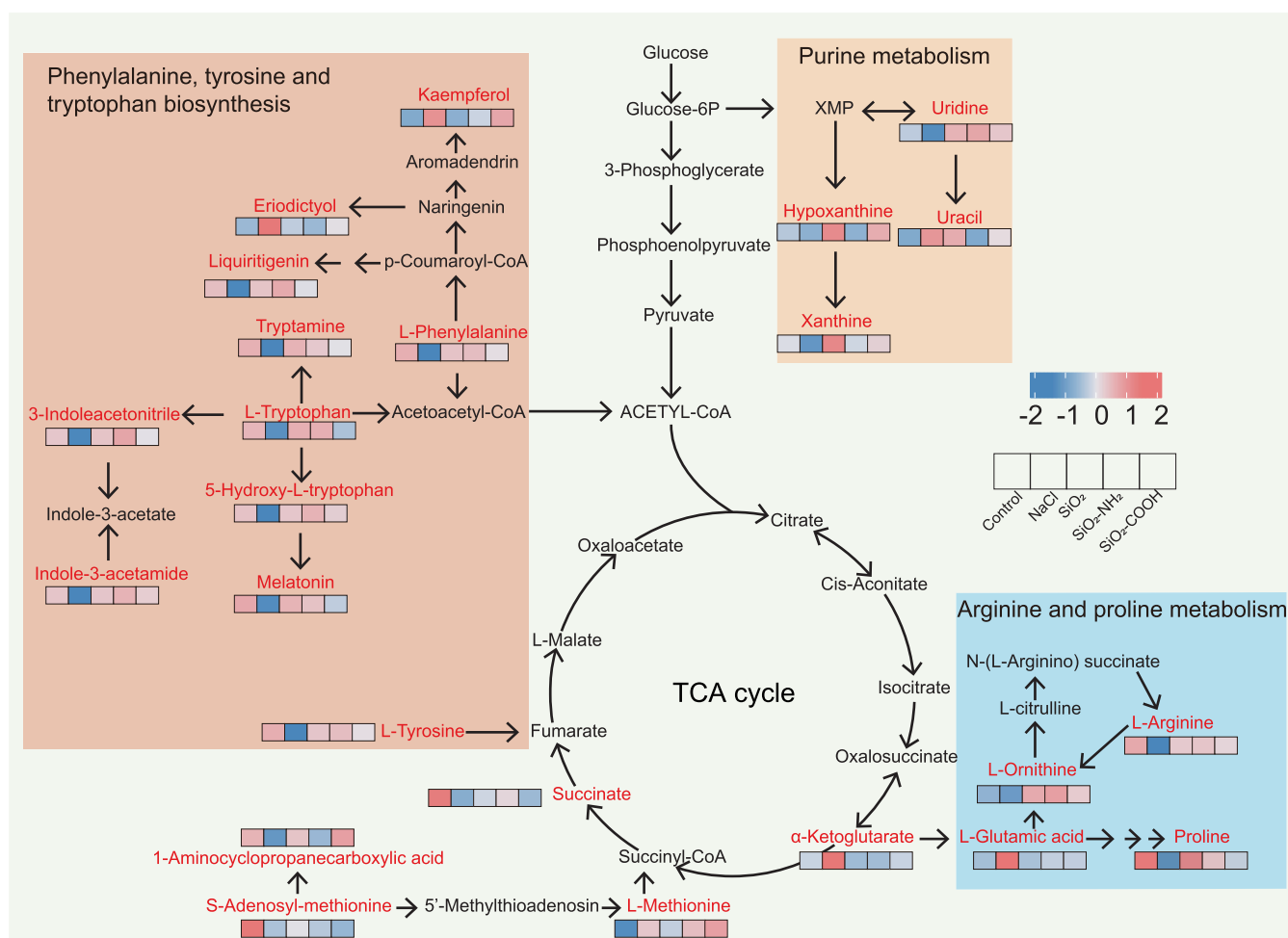


**Figure 3.** Metabolic pathway network signature of primary and secondary metabolites regulated by pristine and functionalized SiO<sub>2</sub> NPs (SiO<sub>2</sub>-NH<sub>2</sub> and SiO<sub>2</sub>-COOH NPs) in soybean roots. The heatmaps of each metabolite were inserted underneath; four boxes from left to right in each row represent the control, NaCl, SiO<sub>2</sub>, SiO<sub>2</sub>-NH<sub>2</sub>, and SiO<sub>2</sub>-COOH, respectively. The log<sub>2</sub> value of the relative content of metabolite in the heatmaps shares the color bar placed on the right of the figure.

rhizosphere microbial communities to different types of SiO<sub>2</sub> NPs (Figures 4 and S7). In the rhizosphere, while the Chao1 and Shannon indices under salt stress did not differ significantly from those of the control, they were significantly reduced with the addition of pristine SiO<sub>2</sub> and SiO<sub>2</sub>-NH<sub>2</sub> NPs (Figure 4A,B). The PCoA analysis showed that all three types of SiO<sub>2</sub> NPs induced significant changes in rhizosphere bacterial community structure compared to the NaCl (ANOSIM,  $p < 0.001$ , Figure 4 C). In this study, pristine and functionalized SiO<sub>2</sub> NPs altered both the structure and composition of both the rhizosphere and endophytic bacterial communities, suggesting that these treatments may help plants recruit specific root-associated bacteria to mitigate salt stress (Figure 4 D). Proteobacteria were notably abundant in both rhizosphere and endosphere samples (Figure S7D), consistent with their role as dominant halophilic/halotolerant phylotypes in saline soils.<sup>68</sup>

A total of 307 bacterial genera were identified, with the 30 most abundant genera selected for further analysis (Figure 4 E). In the rhizosphere, pristine SiO<sub>2</sub> NPs enriched the genus *RB41* (2.52-fold), while SiO<sub>2</sub>-NH<sub>2</sub> NPs enriched both *RB41* (2.58-fold) and *Arthrobacter* (1.69-fold). SiO<sub>2</sub>-COOH treatment resulted in the enrichment of *Arthrobacter* (2.20-fold), *Gaiella* (1.29-fold), and *Rubrobacter* (2.50-fold) in Actino-

bacteria, and *Pseudomonas* (2.81-fold), *Luteimonas* (1.80-fold), *Ellin6067* (1.30-fold), and *Acidibacter* (1.43-fold) in Proteobacteria, *Gemmatimonas* (1.32-fold), and *Haliangium* (1.82-fold). Several of these genera, including *RB41*, *Arthrobacter*, *Ellin6067*, *Gemmatimonas*, and *Haliangium*, were significantly and negatively correlated with the Na<sup>+</sup>/K<sup>+</sup> ratio in soybean roots ( $p < 0.05$ , Figure S8B). These genera are known for their plant growth-promoting activities, such as nitrogen fixation, phosphate solubilization, and production of phytohormones.<sup>69,70</sup> For instance, *Arthrobacter*, frequently found in the rhizosphere of salt-tolerant plants, is known to alleviate salt stress by modulating plant hormone levels,<sup>71</sup> particularly IAA,<sup>72</sup> which helps maintain Na<sup>+</sup>/K<sup>+</sup> homeostasis in plant tissues, thereby enhancing salt tolerance. These findings suggest that functionalized SiO<sub>2</sub> NPs, especially SiO<sub>2</sub>-COOH NPs, may selectively enrich beneficial microbial communities in the rhizosphere, contributing to improved salt tolerance in soybean.

To investigate the functional implications of the observed shifts in rhizosphere microbial communities, we employed PICRUSt2 to predict the functional potential of the bacterial communities based on their 16S rRNA gene profiles (Figures 4 F and S10). Specifically, SiO<sub>2</sub>-COOH NPs treatment significantly upregulated genes related to Na<sup>+</sup> extrusion, K<sup>+</sup>

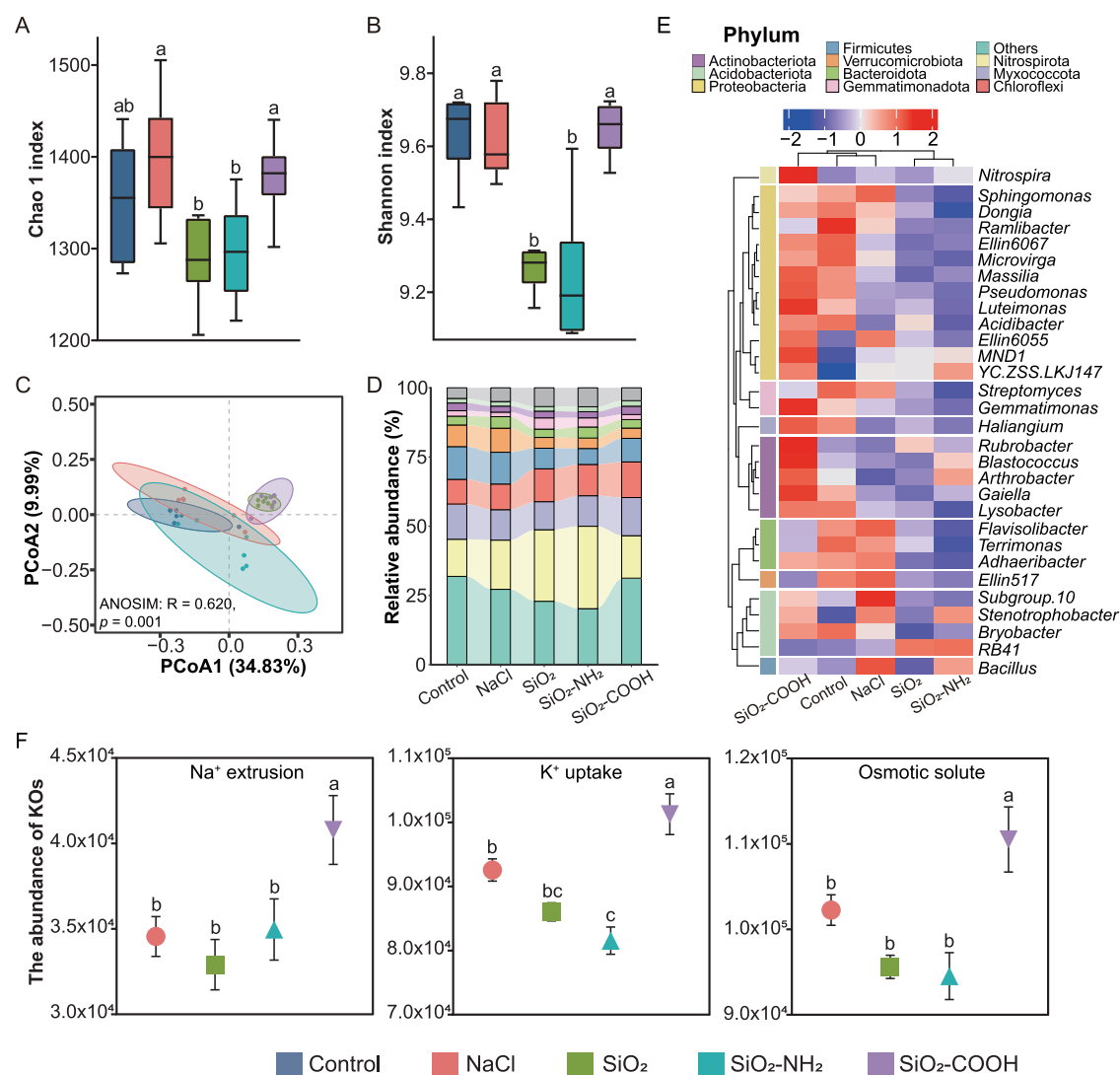


**Figure 4.** Rhizosphere microbial community responses under different treatments. Chao1 (A) and Shannon index (B) of bacterial communities. (C) Principal coordinate analysis (PCoA) of rhizosphere bacterial communities at the ASV level based on the Bray–Curtis distance. Different ellipses represent 95% confidence intervals from five treatment samples, respectively. (D) Relative abundance at the phylum level. (E) Heat map of the top 30 genera. (F) Differences in salt-resistance genes of rhizosphere bacteria. Letters indicate significant differences among different treatments at the  $p < 0.05$  level (one-way ANOVA). Control: nonsalt stress, NaCl: salt stress, SiO<sub>2</sub>: pristine SiO<sub>2</sub> NPs + salt stress, SiO<sub>2</sub>-NH<sub>2</sub>: SiO<sub>2</sub>-NH<sub>2</sub> NPs + salt stress, SiO<sub>2</sub>-COOH: SiO<sub>2</sub>-COOH NPs + salt stress.

uptake, and osmotic solute accumulation compared to NaCl, pristine SiO<sub>2</sub>, and SiO<sub>2</sub>-NH<sub>2</sub> NPs. The enhanced Na<sup>+</sup> extrusion capacity in the rhizosphere could contribute to a more efficient exclusion of Na<sup>+</sup> from the root zone, mitigating the detrimental effects of Na<sup>+</sup> toxicity on plant cells.<sup>73</sup> Simultaneously, the upregulation of K<sup>+</sup> uptake genes could improve K<sup>+</sup> acquisition by plants, helping maintain a favorable cytosolic K<sup>+</sup>/Na<sup>+</sup> ratio essential for various cellular processes under salt stress.<sup>74</sup> Furthermore, the increased expression of genes related to osmolyte accumulation, such as proline and glycine betaine biosynthesis, could enhance the production of osmoprotectants by rhizosphere microbes.<sup>75</sup> These osmoprotectants can then be taken up by plants, contributing to osmotic adjustment and cellular protection under salt stress.<sup>76</sup> The observed enrichment of specific metabolic pathways under SiO<sub>2</sub>-COOH NPs treatment compared with NaCl, as revealed by STAMP analysis, further strengthens the link between rhizosphere microbiome function and soybean salt tolerance (Figure S10). For instance, the enrichment of arginine and

proline metabolism could contribute to enhanced osmoregulation in soybean under salt stress, as both arginine and proline are important precursors for the synthesis of osmoprotectants.<sup>60</sup> In addition, functional expressions, such as biofilm formation and flagellar assembly, were also significantly enriched. These functional changes in the rhizosphere microbiome, coupled with the increased abundance of beneficial bacteria such as *Arthrobacter* and *Pseudomonas*, likely contribute to the enhanced salt tolerance observed in SiO<sub>2</sub>-COOH-treated plants. This highlights the potential of SiO<sub>2</sub>-COOH NPs, to not only shape the structure of the rhizosphere microbiome but also modulate its function in a way that benefits plant growth and stress tolerance. For more details on changes in the structure and function of bacterial communities within roots, see the Text S5.

**Soil Nutrients.** To evaluate the effect of SiO<sub>2</sub> NPs addition on soil nutrient availability under salt stress, we measured soil NH<sub>4</sub><sup>+</sup>-N, NO<sub>3</sub><sup>-</sup>-N, AK, SOM, and AP contents under different treatments. After 30 days of planting, the AK and AP contents

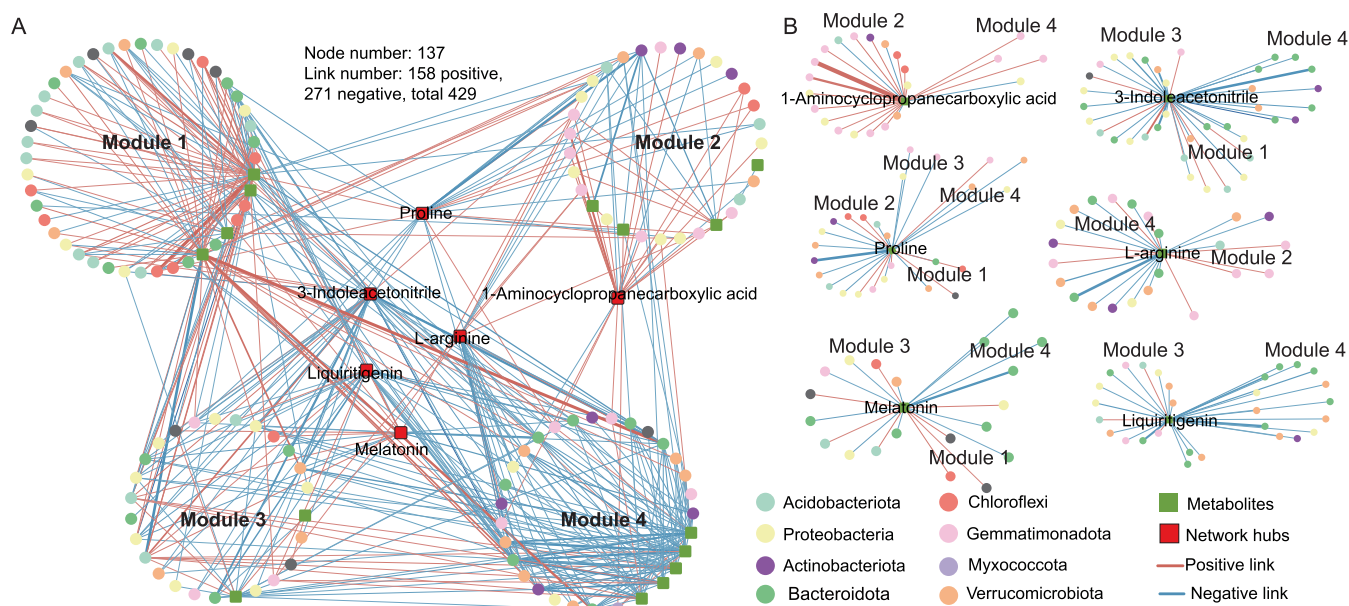


**Figure 5.** Co-occurrence network of soybean metabolites and microbial ASVs exposed to three NPs treatments. (A) Association network between 116 16S ASVs and 21 DEMs. Nodes with circle symbols represent 16S ASVs, and nodes with square symbols represent metabolites. Links between nodes are based on Spearman correlations ( $r > 0.6$ ,  $p < 0.05$ ) of their relative abundances, red for positive correlation and blue for negative correlation. The network separates into four modules shown as the four numbered circles. Red-filled squares highlight metabolites that act as network hubs, which are the nodes with dense connections to other nodes within the entire network. (B) Subnetworks of metabolites that formed network hubs and their neighboring microbial nodes. Microbial ASVs are colored by class for Proteobacteria and by phylum for all other phyla.

of soil were significantly reduced by 13.5% and 19.3% under salt stress, compared to the control (Figure S12C–E). The addition of both pristine and functionalized SiO<sub>2</sub> NPs significantly altered soil nutrient content under salt stress. Notably, SiO<sub>2</sub>-COOH NPs resulted in significant increases in NH<sub>4</sub><sup>+</sup>-N (259.7%), and NO<sub>3</sub><sup>-</sup>-N (35.1%) compared to the NaCl treatment. In addition, SOM, AK, and AP contents also increased significantly under SiO<sub>2</sub> NPs treatments. Metabolomics analysis of root exudates revealed a significant enrichment of amino acid metabolic pathways and increased secretion of several amino acids under SiO<sub>2</sub>-COOH NPs treatment (Figures 3, S4, and S5). These amino acids could serve as substrates for microbial nitrogen cycling processes, such as ammonification and nitrification.<sup>77,78</sup> Furthermore, SiO<sub>2</sub>-COOH NPs enriched several bacterial genera known to be involved in nitrogen cycling, such as *Arthrobacter*, *Pseudomonas*, and *Gaiella* (Figure 4). The enrichment of these genera in the rhizosphere of SiO<sub>2</sub>-COOH NPs treated plants could have enhanced the mineralization of organic nitrogen in the soil, making it more available as NH<sub>4</sub><sup>+</sup>-N and NO<sub>3</sub><sup>-</sup>-N.<sup>79,80</sup> In contrast, pristine SiO<sub>2</sub> NPs mainly enhanced available phosphorus (AP) by 163.7%, while SiO<sub>2</sub>-NH<sub>2</sub> NPs notably increased NH<sub>4</sub><sup>+</sup>-N by 105.3% (Figure S12A). These results highlight the enhanced impact of SiO<sub>2</sub>-COOH NPs on improving nitrogen availability, which is critical for plant growth under salt stress conditions.<sup>81</sup> Nutrients, such as nitrogen and phosphorus, are vital for plant growth and stress resilience. P is essential for root development and energy metabolism, while N is key to protein synthesis and chlorophyll formation, which in turn increases photosynthesis.<sup>82</sup> Zhang et al.<sup>83</sup> found that N supplementation led to increased proline and chlorophyll accumulation, reduced malondialdehyde levels, as well as regulated hormone homeostasis, thereby improving the salt tolerance of grape seedlings.

### Metabolite-Microbe Rhizosphere Network Interactions.

Taxon-specific responses to individual rhizosphere metabolites could be an important driver of the rhizosphere bacterial community assembly. Therefore, co-occurrence network analysis was employed to explore the complex interplay between root exudate metabolites and rhizosphere microbial communities under SiO<sub>2</sub> NPs treatment. In the constructed network of rhizosphere ASVs and DEMs (Figure 5 A), 116 ASVs were connected to 21 metabolites via 429 links, comprising 158 positive and 271 negative correlations. This intricate network structure highlights the potential for extensive interactions between root-derived metabolites and rhizosphere microbes. Six metabolites were identified as putative keystone metabolites based on their high centrality within the network (Figure 5 B). Five of these keystone metabolites, namely, 3-indoleacetonitrile, proline, L-arginine, melatonin, and liquiritigenin, were predominantly involved in negative correlations with bacterial ASVs. Liquiritigenin, a flavonoid with diverse biological activities,<sup>84</sup> exhibited negative correlations with a large proportion (89.65%) of the connected bacterial ASVs. This suggests that liquiritigenin may play a role in shaping rhizosphere microbial communities by selectively inhibiting the growth of certain bacterial taxa. In contrast, 1-aminocyclopropanecarboxylic acid (ACC), the immediate precursor of the plant hormone ethylene,<sup>85</sup> exhibited predominantly positive correlations (81.8%) with bacterial ASVs, suggesting a potential role in promoting the growth of specific bacterial taxa. Module 1, the largest module within the network, was driven by positive interactions with L-tryptophan, an essential amino acid and precursor for various plant metabolites, including the phytohormone IAA.<sup>64</sup> L-tryptophan exhibited positive associations with 71.9% of the connected bacterial ASVs of diverse lineages, suggesting its potential role as a key driver of microbial community assembly in the rhizosphere. These findings underscore the complex and

multifaceted interactions between root exudates and the rhizosphere microbiome, highlighting the potential for specific metabolites to act as key regulators of the microbial community structure and function.

In these association networks, we found that half of the six module hubs were organic acids, with proline possessing the most links to microbial ASVs of the three (Figure 5). It has been shown that organic acids, and in particular amino acids, are exuded by plants as they develop, and that greater abundances of such acids correspond to large-scale shifts in soil microbial community composition.<sup>86</sup> Several potential mechanisms of how amino acids may modulate rhizomicrobiomes have been proposed, including shifts in soil pH, antimicrobial effects, or preferential utilization of these metabolites as a nutrient source by specific microbial taxa geared to decompose them.<sup>87</sup> It is notable given that organic acids are among the dominant classes of exudate compounds and many plants are known to exude them (along with other rhizodeposits) from their roots during active growth and development.<sup>88</sup> Thus, amino acids such as 1-Aminocyclopropanecarboxylic acid and proline are likely strong drivers of the switchgrass rhizomicrobiome structure.

This study demonstrates the significant potential of functionalized SiO<sub>2</sub> NPs, particularly SiO<sub>2</sub>-COOH NPs, in enhancing soybean tolerance to salt stress through multifaceted interactions with plant physiology and the rhizosphere microbiome. Our findings show that soybean growth and development were inhibited under salt stress, and the application of SiO<sub>2</sub>-COOH NPs significantly alleviated these negative effects. Specifically, SiO<sub>2</sub>-COOH NPs promoted root development, resulting in a more extensive root system that facilitated improved nutrient and water uptake. These NPs also altered root exudation patterns, increasing the secretion of beneficial compounds such as L-tryptophan, tryptophan, and indole-3-acetamide, which likely stimulated the recruitment and colonization of beneficial microbes. Furthermore, SiO<sub>2</sub>-COOH NPs reshaped the rhizosphere microbiome, enriching beneficial microbes with plant growth-promoting traits like IAA production and nutrient acquisition. The superior efficacy of SiO<sub>2</sub>-COOH NPs compared to pristine SiO<sub>2</sub> NPs underscores the importance of surface functionalization in optimizing nanoparticle performance for agricultural applications. These results highlight the promising potential of SiO<sub>2</sub>-COOH NPs as a nanobio-stimulant, providing eco-friendly and sustainable solutions to enhance crop resilience and productivity in salt-affected regions. However, given the short experimental duration, use of a single soybean variety, and controlled growth conditions, further research under diverse field environments and crop systems is necessary to validate their broader applicability.

## ■ ASSOCIATED CONTENT

### SI Supporting Information

The Supporting Information is available free of charge at <https://pubs.acs.org/doi/10.1021/acs.jafc.5c00194>.

Transmission electron micrographs of images of pristine SiO<sub>2</sub> NPs and functionalized SiO<sub>2</sub> NPs; SPAD and the roots and shoots Si content; metabolic analysis of soybean root; significant enriched KEGG pathways; cumulative secretion level of soybean root exudate; characteristics of endosphere microbial community structure; correlation of bacterial genera with Na<sup>+</sup>/K<sup>+</sup>;

extended error bar plot of differentially abundant KEGG pathways of rhizosphere bacteria; extended error bar plot of differentially abundant KEGG pathways of endosphere bacteria; the NH<sub>4</sub><sup>+</sup>-N, NO<sub>3</sub><sup>-</sup>-N, AK, SOM, AP content in soil; PCR amplification reaction system and conditions of bacteria; differences in significantly altered bacterial community structure between pairwise treatments based on ANOSIM; and KOs related to Na<sup>+</sup> extrusion, K<sup>+</sup> uptake and osmotic solute (PDF)

## ■ AUTHOR INFORMATION

### Corresponding Authors

**Gehong Wei** – State Key Laboratory for Crop Stress Resistance and High-Efficiency Production, Shaanxi Key Laboratory of Agricultural and Environmental Microbiology, College of Life Sciences, Northwest A&F University, Yangling 712100 Shaanxi, China; Email: [weigehong@nwsuaf.edu.cn](mailto:weigehong@nwsuaf.edu.cn)

**Chun Chen** – State Key Laboratory for Crop Stress Resistance and High-Efficiency Production, Shaanxi Key Laboratory of Agricultural and Environmental Microbiology, College of Life Sciences, Northwest A&F University, Yangling 712100 Shaanxi, China; [orcid.org/0000-0001-7246-7281](https://orcid.org/0000-0001-7246-7281); Email: [chunchen@nwsuaf.edu.cn](mailto:chunchen@nwsuaf.edu.cn)

### Authors

**Zhidi Chen** – State Key Laboratory for Crop Stress Resistance and High-Efficiency Production, Shaanxi Key Laboratory of Agricultural and Environmental Microbiology, College of Life Sciences, Northwest A&F University, Yangling 712100 Shaanxi, China; [orcid.org/0000-0003-3894-0252](https://orcid.org/0000-0003-3894-0252)

**Pan Wang** – State Key Laboratory for Crop Stress Resistance and High-Efficiency Production, Shaanxi Key Laboratory of Agricultural and Environmental Microbiology, College of Life Sciences, Northwest A&F University, Yangling 712100 Shaanxi, China; College of Tea Science, Xinyang Agriculture and Forestry University, Xinyang 464000 Henan, China; [orcid.org/0000-0002-6476-5358](https://orcid.org/0000-0002-6476-5358)

**Simin Zhao** – State Key Laboratory for Crop Stress Resistance and High-Efficiency Production, Shaanxi Key Laboratory of Agricultural and Environmental Microbiology, College of Life Sciences, Northwest A&F University, Yangling 712100 Shaanxi, China; College of Natural Resources and Environment, Northwest A&F University, Yangling 712100 Shaanxi, China

**Yangping Sun** – State Key Laboratory for Crop Stress Resistance and High-Efficiency Production, Shaanxi Key Laboratory of Agricultural and Environmental Microbiology, College of Life Sciences, Northwest A&F University, Yangling 712100 Shaanxi, China

**Yidan Liu** – State Key Laboratory for Crop Stress Resistance and High-Efficiency Production, Shaanxi Key Laboratory of Agricultural and Environmental Microbiology, College of Life Sciences, Northwest A&F University, Yangling 712100 Shaanxi, China

**Sanfeng Chen** – State Key Laboratory for Agrobiotechnology, College of Biological Sciences, China Agricultural University, Beijing 100193, China; [orcid.org/0000-0003-2956-9025](https://orcid.org/0000-0003-2956-9025)

**Wenfeng Chen** – State Key Laboratory of Agrobiotechnology, College of Biological Sciences and Rhizobium Research Center, China Agricultural University, Beijing 100193, China

**Gangyong Zhao** – Tianjin Kunhe Bio-technology Group Co., Ltd., Tianjin 300450, China

Complete contact information is available at:  
<https://pubs.acs.org/10.1021/acs.jafc.5c00194>

### Author Contributions

<sup>V</sup>Z.C. and P.W. are co-first authors who contributed equally to this work. Z.C.: investigation, data curation, visualization, formal analysis, writing – original draft, writing – review and editing. P.W.: methodology, investigation, visualization. S.Z.: investigation, and visualization. Y.S.: investigation and visualization. Y.L.: investigation and visualization. S.C.: investigation. W.C.: investigation. G.Z.: investigation. G.W.: resources, supervision, validation, and project administration. C.C.: conceptualization, methodology, funding acquisition, supervision, project administration, and writing – review and editing.

### Notes

The authors declare no competing financial interest.

### ACKNOWLEDGMENTS

This work was supported by the National Natural Science Foundation of China (42277118) and the National Key Research and Development Program of China (2023YFD1900901).

### REFERENCES

- (1) Balasubramaniam, T.; Shen, G.; Esmaeili, N.; Zhang, H. Plants' response mechanisms to salinity stress. *Plants* **2023**, *12* (12), 2253.
- (2) Ismail, A.; Takeda, S.; Nick, P. Life and death under salt stress: Same players, different timing? *J. Exp. Bot.* **2014**, *65* (12), 2963–2979.
- (3) Rizwan, A.; Zia-ur-Rehman, M.; Rizwan, M.; Usman, M.; Anayatullah, S.; Areej; Alharby, H. F.; Bamagoos, A. A.; Alharbi, B. M.; Ali, S. Effects of silicon nanoparticles and conventional Si amendments on growth and nutrient accumulation by maize (*Zea mays* L.) grown in saline-sodic soil. *Environ. Res.* **2023**, *227*, No. 115740.
- (4) Ju, F.; Pang, J.; Sun, L.; Gu, J.; Wang, Z.; Wu, X.; Ali, S.; Wang, Y.; Zhao, W.; Wang, S.; Zhou, Z.; Chen, B. Integrative transcriptomic, metabolomic and physiological analyses revealed the physiological and molecular mechanisms by which potassium regulates the salt tolerance of cotton (*Gossypium hirsutum* L.) roots. *Ind. Crops Prod.* **2023**, *193*, No. 116177.
- (5) Zou, J.; Yu, H.; Yu, Q.; Jin, X.; Cao, L.; Wang, M.; Wang, M.; Ren, C.; Zhang, Y. Physiological and UPLC-MS/MS widely targeted metabolites mechanisms of alleviation of drought stress-induced soybean growth inhibition by melatonin. *Ind. Crops Prod.* **2021**, *163*, No. 113323.
- (6) Mirza, H.; Khursheda, P.; Taufika Islam, A.; Abdul Awal Chowdhury, M.; Farzana, N. Salt Stress Responses and Tolerance in Soybean. In *Plant Stress Physiology*; Mirza, H.; Kamran, N., Eds.; IntechOpen: Rijeka, 2022; Chapter 3.
- (7) Wang, P.; Zhang, H.; Hu, X.; Xu, L.; An, X.; Jin, T.; Ma, R.; Li, Z.; Chen, S.; Du, S.; Wei, G.; Chen, C. Comparing the potential of silicon nanoparticles and conventional silicon for salinity stress alleviation in soybean (*Glycine max* L.): Growth and physiological traits and rhizosphere/endophytic bacterial communities. *J. Agric. Food Chem.* **2024**, *72* (19), 10781–10793.
- (8) Guan, R.; Guo, X.; Qu, Y.; Zhang, Z.; Bao, L.; Ye, R.; Chang, R.; Qiu, L. Salt tolerance in soybeans: Focus on screening methods and genetics. *Plants* **2024**, *13* (1), No. 97, DOI: 10.3390/plants13010097.
- (9) Wang, M.; Wang, R.; Mur, L. A. J.; Ruan, J.; Shen, Q.; Guo, S. Functions of silicon in plant drought stress responses. *Hortic. Res.* **2021**, *8* (1), 254.
- (10) Kafi, M.; Rahimi, Z. Effect of salinity and silicon on root characteristics, growth, water status, proline content and ion accumulation of purslane (*Portulaca oleracea* L.). *Soil Sci. Plant Nutr.* **2011**, *57* (2), 341–347.
- (11) Souri, Z.; Khanna, K.; Karimi, N.; Ahmad, P. Silicon and plants: Current knowledge and future prospects. *J. Plant Growth Regul.* **2021**, *40* (3), 906–925.
- (12) Zhao, P.; Cao, L.; Ma, D.; Zhou, Z.; Qi, H.; Pan, C. Translocation, distribution and degradation of prochloraz-loaded mesoporous silica nanoparticles in cucumber plant. *Nanoscale* **2017**, *10*, 1798–1806, DOI: 10.1039/C7NR08107C.
- (13) Alsaeedi, A. H.; El-Ramady, H.; Alshaal, T.; El-Garawani, M.; Elhawat, N.; Almohsen, M. Engineered silica nanoparticles alleviate the detrimental effects of Na<sup>+</sup> stress on germination and growth of common bean (*Phaseolus vulgaris*). *Environ. Sci. Pollut. Res.* **2017**, *24* (27), 21917–21928.
- (14) Kostic, L.; Nikolic, N.; Bosnic, D.; Samardzic, J.; Nikolic, M. Silicon increases phosphorus (P) uptake by wheat under low P acid soil conditions. *Plant Soil* **2017**, *419* (1), 447–455.
- (15) Alam, P.; Arshad, M.; Al-Kheraif, A. A.; Azzam, M. A.; Al Balawi, T. Silicon nanoparticle-induced regulation of carbohydrate metabolism, photosynthesis, and ROS homeostasis in solanum lycopersicum subjected to salinity stress. *ACS Omega* **2022**, *7* (36), 31834–31844.
- (16) Santana, I.; Wu, H.; Hu, P.; Giraldo, J. P. Targeted delivery of nanomaterials with chemical cargoes in plants enabled by a biorecognition motif. *Nat. Commun.* **2020**, *11* (1), No. 2045.
- (17) Neamtu, M.; Nadejde, C.; Hodoroaba, V.-D.; Schneider, R. J.; Verestiuc, L.; Panne, U. Functionalized magnetic nanoparticles: Synthesis, characterization, catalytic application and assessment of toxicity. *Sci. Rep.* **2018**, *8* (1), No. 6278.
- (18) Rasmussen, M. K.; Pedersen, J. N.; Marie, R. Size and surface charge characterization of nanoparticles with a salt gradient. *Nat. Commun.* **2020**, *11* (1), No. 2337.
- (19) Chen, L.; Zhu, L.; Cheng, H.; Xu, W.; Li, G.; Zhang, Y.; Gu, J.; Chen, L.; Xie, Z.; Li, Z.; Wu, H. Negatively charged carbon dots employed symplastic and apoplastic pathways to enable better plant delivery than positively charged carbon dots. *ACS Nano* **2024**, *18* (34), 23154–23167.
- (20) Hu, P.; An, J.; Faulkner, M. M.; Wu, H.; Li, Z.; Tian, X.; Giraldo, J. P. Nanoparticle charge and size control foliar delivery efficiency to plant cells and organelles. *ACS Nano* **2020**, *14* (7), 7970–7986.
- (21) Rosen, J. E.; Gu, F. X. Surface functionalization of silica nanoparticles with cysteine: A low-fouling zwitterionic surface. *Langmuir* **2011**, *27* (17), 10507–10513.
- (22) Vandenkoornhuysen, P.; Quaiser, A.; Duhamel, M.; Le Van, A.; Dufresne, A. The importance of the microbiome of the plant holobiont. *New Phytol.* **2015**, *206* (4), 1196–1206.
- (23) Trivedi, P.; Leach, J. E.; Tringe, S. G.; Sa, T.; Singh, B. K. Plant–microbiome interactions: from community assembly to plant health. *Nat. Rev. Microbiol.* **2020**, *18* (11), 607–621.
- (24) Bilal, S.; Shahzad, R.; Imran, M.; Jan, R.; Kim, K. M.; Lee, I.-J. Synergistic association of endophytic fungi enhances *Glycine max* L. resilience to combined abiotic stresses: Heavy metals, high temperature and drought stress. *Ind. Crops Prod.* **2020**, *143*, No. 111931.
- (25) Schmitz, L.; Yan, Z.; Schneiderberg, M.; de Roij, M.; Pijnenburg, R.; Zheng, Q.; Franken, C.; Dechesne, A.; Trindade, L. M.; van Velzen, R.; Bisseling, T.; Geurts, R.; Cheng, X. Synthetic bacterial community derived from a desert rhizosphere confers salt stress resilience to tomato in the presence of a soil microbiome. *ISME J.* **2022**, *16* (8), 1907–1920.
- (26) Wang, Y.; Sun, Q.; Liu, J.; Wang, L.; Wu, X.; Zhao, Z.; Wang, N.; Gao, Z. Sueda salsa root-associated microorganisms could effectively improve maize growth and resistance under salt stress. *Microbiol. Spectrum* **2022**, *10* (4), No. e01349-22.
- (27) Yasmin, H.; Naeem, S.; Bakhtawar, M.; Jabeen, Z.; Nosheen, A.; Naz, R.; Keyani, R.; Mumtaz, S.; Hassan, M. N. Halotolerant rhizobacteria *Pseudomonas pseudoalcaligenes* and *Bacillus subtilis* mediate systemic tolerance in hydroponically grown soybean (*Glycine max* L.) against salinity stress. *PLoS One* **2020**, *15* (4), No. e0231348.

- (28) Akhtar, N.; Ilyas, N.; Mashwani, Z.-u.-R.; Hayat, R.; Yasmin, H.; Noureldeen, A.; Ahmad, P. Synergistic effects of plant growth promoting rhizobacteria and silicon dioxide nano-particles for amelioration of drought stress in wheat. *Plant Physiol. Biochem.* **2021**, *166*, 160–176.
- (29) Das, S.; Gwon, H. S.; Khan, M. I.; Van Nostrand, J. D.; Alam, M. A.; Kim, P. J. Taxonomic and functional responses of soil microbial communities to slag-based fertilizer amendment in rice cropping systems. *Environ. Int.* **2019**, *127*, 531–539.
- (30) Hiebner, D. W.; Barros, C.; Quinn, L.; Vitale, S.; Casey, E. Surface functionalization-dependent localization and affinity of SiO<sub>2</sub> nanoparticles within the biofilm EPS matrix. *Biofilm* **2020**, *2*, No. 100029.
- (31) Rehman, S.; Khan, K.; Mujahid, M.; Nosheen, S. Synthesis of nano-hydroxyapatite and its rapid mediated surface functionalization by silane coupling agent. *Mater. Sci. Eng. C* **2016**, *58*, 675–681.
- (32) Shen, Z.; Pu, X.; Wang, S.; Dong, X.; Cheng, X.; Cheng, M. Silicon improves ion homeostasis and growth of liquorice under salt stress by reducing plant Na<sup>+</sup> uptake. *Sci. Rep.* **2022**, *12* (1), No. 5089.
- (33) Alsaeedi, A.; El-Ramady, H.; Alshaal, T.; El-Garawany, M.; Elhawati, N.; Al-Otaibi, A. Silica nanoparticles boost growth and productivity of cucumber under water deficit and salinity stresses by balancing nutrients uptake. *Plant Physiol. Biochem.* **2019**, *139*, 1–10.
- (34) Barros, J. A. V. A.; de Souza, P. F.; Schiavo, D.; Nóbrega, J. A. Microwave-assisted digestion using diluted acid and base solutions for plant analysis by ICP OES. *J. Anal. At. Spectrom.* **2016**, *31* (1), 337–343.
- (35) Zhao, M.; Zhao, J.; Yuan, J.; Hale, L.; Wen, T.; Huang, Q.; Vivanco, J. M.; Zhou, J.; Kowalchuk, G. A.; Shen, Q. Root exudates drive soil-microbe-nutrient feedbacks in response to plant growth. *Plant, Cell Environ.* **2021**, *44* (2), 613–628.
- (36) Olsen, S. R. *Estimation of Available Phosphorus in Soils by Extraction with Sodium Bicarbonate* U.S. Government; 1954.
- (37) Yu, W.; Huang, W.; Weintraub-Leff, S. R.; Hall, S. J. Where and why do particulate organic matter (POM) and mineral-associated organic matter (MAOM) differ among diverse soils? *Soil Biol. Biochem.* **2022**, *172*, No. 108756, DOI: 10.1016/j.soilbio.2022.108756.
- (38) Chaparro, J. M.; Badri, D. V.; Vivanco, J. M. Rhizosphere microbiome assemblage is affected by plant development. *ISME J.* **2014**, *8* (4), 790–803.
- (39) Xiong, C.; Zhu, Y.; Wang, J.; Singh, B.; Han, L.; Shen, J.; Li, P.; Wang, G.; Wu, C.; Ge, A.; Zhang, L.; He, J. Host selection shapes crop microbiome assembly and network complexity. *New Phytol.* **2021**, *229* (2), 1091–1104.
- (40) Li, H.; Rao, Z.; Sun, G.; Wang, M.; Yang, Y.; Zhang, J.; Li, H.; Pan, M.; Wang, J.-J.; Chen, X. W. Root chemistry and microbe interactions contribute to metal (loid) tolerance of an aromatic plant-Vetiver grass. *J. Hazard. Mater.* **2024**, *461*, No. 132648, DOI: 10.1016/j.jhazmat.2023.132648.
- (41) Liu, L.; Tsyusko, O. V.; Unrine, J. M.; Liu, S.; Liu, Y.; Guo, L.; Wei, G.; Chen, C. Pristine and sulfidized Zinc Oxide nanoparticles promote the release and decomposition of organic carbon in the legume rhizosphere. *Environ. Sci. Technol.* **2023**, *57* (24), 8943–8953.
- (42) Prasad, T. N. V. K. V.; Swethasree, M.; Satisha, G. C.; Nirmal Kumar, A. R.; Sudhakar, P.; Ravindra Reddy, B.; Saritha, M.; Sabitha, N.; Bhaskar Reddy, B. V.; Rajasekhar, P.; Prasanthi, L.; Girish, B. P.; Roy Choudhury, S. Nanoparticulate silica internalization and its effect on the growth and yield of groundnut (*Arachis hypogaea* L.). *Environ. Sci. Technol.* **2023**, *57* (14), 5881–5890.
- (43) Zhu, J.; Liu, S.; Wang, H.; Wang, D.; Zhu, Y.; Wang, J.; He, Y.; Zheng, Q.; Zhan, X. Microplastic particles alter wheat rhizosphere soil microbial community composition and function. *J. Hazard. Mater.* **2022**, *436*, No. 129176.
- (44) Zhang, H.; Huang, M.; Zhang, W.; Gardea-Torresdey, J. L.; White, J. C.; Ji, R.; Zhao, L. Silver nanoparticles alter soil microbial community compositions and metabolite profiles in unplanted and cucumber-planted soils. *Environ. Sci. Technol.* **2020**, *54* (6), 3334–3342.
- (45) Liu, X.; Liu, H.; Zhang, Y.; Chen, G.; Li, Z.; Zhang, M. Straw return drives soil microbial community assemblage to change metabolic processes for soil quality amendment in a rice-wheat rotation system. *Soil Biol. Biochem.* **2023**, *185*, No. 109131, DOI: 10.1016/j.soilbio.2023.109131.
- (46) Chen, S.; Waghmode, T. R.; Sun, R.; Kuramae, E. E.; Hu, C.; Liu, B. Root-associated microbiomes of wheat under the combined effect of plant development and nitrogen fertilization. *Microbiome* **2019**, *7* (1), 136.
- (47) Guimerà, R.; Nunes Amaral, L. A. Functional cartography of complex metabolic networks. *Nature* **2005**, *433* (7028), 895–900.
- (48) Luo, X.; Wang, Z.; Wang, C.; Yue, L.; Tao, M.; Elmer, W. H.; White, J. C.; Cao, X.; Xing, B. Nanomaterial size and surface modification mediate disease resistance activation in Cucumber (*Cucumis sativus*). *ACS Nano* **2023**, *17* (5), 4871–4885.
- (49) Qados, A. M. S. A.; Moftah, A. E. Influence of silicon and nano-silicon on germination, growth and yield of faba bean (*Vicia faba* L.) under salt stress conditions. *J. Exp. Agric. Int.* **2015**, *5* (6), 509–524.
- (50) Acosta-Motos, J. R.; Ortuño, M. F.; Bernal-Vicente, A.; Diaz-Vivancos, P.; Sanchez-Blanco, M. J.; Hernandez, J. A. Plant responses to salt stress: Adaptive mechanisms. *Agronomy* **2017**, *7* (1), 18.
- (51) Lu, X.; Sun, D.; Zhang, X.; Hu, H.; Kong, L.; Rookes, J. E.; Xie, J.; Cahill, D. M. Stimulation of photosynthesis and enhancement of growth and yield in *Arabidopsis thaliana* treated with amine-functionalized mesoporous silica nanoparticles. *Plant Physiol. Biochem.* **2020**, *156*, 566–577.
- (52) Hameed, A.; Ahmed, M. Z.; Hussain, T.; Aziz, I.; Ahmad, N.; Gul, B.; Nielsen, B. L. Effects of salinity stress on chloroplast structure and function. *Cells* **2021**, *10* (8), No. 2023, DOI: 10.3390/cells10082023.
- (53) Zhou, H.; Shi, H.; Yang, Y.; Feng, X.; Chen, X.; Xiao, F.; Lin, H.; Guo, Y. Insights into plant salt stress signaling and tolerance. *J. Genet. Genomics* **2024**, *51* (1), 16–34.
- (54) Dong, H.; Wang, Y.; Di, Y.; Qiu, Y.; Ji, Z.; Zhou, T.; Shen, S.; Du, N.; Zhang, T.; Dong, X.; Guo, Z.; Piao, F.; Li, Y. Plant growth-promoting rhizobacteria *Pseudomonas aeruginosa* HG28–5 improves salt tolerance by regulating Na<sup>+</sup>/K<sup>+</sup> homeostasis and ABA signaling pathway in tomato. *Microbiol. Res.* **2024**, *283*, No. 127707.
- (55) Ijaz, U.; Ahmed, T.; Rizwan, M.; Noman, M.; Shah, A. A.; Azeem, F.; Alharby, H. F.; Bamagoos, A. A.; Alharbi, B. M.; Ali, S. Rice straw based silicon nanoparticles improve morphological and nutrient profile of rice plants under salinity stress by triggering physiological and genetic repair mechanisms. *Plant Physiol. Biochem.* **2023**, *201*, No. 107788.
- (56) Gohari, G.; Panahirad, S.; Sadeghi, M.; Akbari, A.; Zareei, E.; Zahedi, S. M.; Bahrami, M. K.; Fotopoulos, V. Putrescine-functionalized carbon quantum dot (put-CQD) nanoparticles effectively prime grapevine (*Vitis vinifera* cv. Sultana) against salt stress. *BMC Plant Biol.* **2021**, *21* (1), 120.
- (57) Cao, L.; Chen, I. C.; Li, Z.; Liu, X.; Mubashir, M.; Nuaimi, R. A.; Lai, Z. Switchable Na<sup>+</sup> and K<sup>+</sup> selectivity in an amino acid functionalized 2D covalent organic framework membrane. *Nat. Commun.* **2022**, *13* (1), No. 7894.
- (58) Chai, Y. N.; Schachtman, D. P. Root exudates impact plant performance under abiotic stress. *Trends Plant Sci.* **2022**, *27* (1), 80–91.
- (59) Singh, P.; Choudhary, K. K.; Chaudhary, N.; Gupta, S.; Sahu, M.; Tejaswini, B.; Sarkar, S. Salt stress resilience in plants mediated through osmolyte accumulation and its crosstalk mechanism with phytohormones. *Front. Plant Sci.* **2022**, *13*, No. 1006617.
- (60) Zhang, H.; Zhu, J.; Gong, Z.; Zhu, J.-K. Abiotic stress responses in plants. *Nat. Rev. Genet.* **2022**, *23* (2), 104–119.
- (61) Llebrés, M.-T.; Pascual, M.-B.; Debille, S.; Trontin, J.-F.; Harvengt, L.; Avila, C.; Cánovas, F. M. The role of arginine metabolic pathway during embryogenesis and germination in maritime pine (*Pinus pinaster* Ait.). *Tree Physiol.* **2018**, *38* (3), 471–484.
- (62) Patel, M. K.; Kumar, M.; Li, W.; Luo, Y.; Burritt, D. J.; Alkan, N.; Tran, L.-S. P. Enhancing salt tolerance of plants: From metabolic

reprogramming to exogenous chemical treatments and molecular approaches. *Cells* **2020**, *9* (11), 2492.

(63) Wang, B.; Zhang, H.; Huai, J.; Peng, F.; Wu, J.; Lin, R.; Fang, X. Condensation of SEUSS promotes hyperosmotic stress tolerance in *Arabidopsis*. *Nat. Chem. Biol.* **2022**, *18* (12), 1361–1369.

(64) Corpas, F.; Gupta, D.; Palma, J. *Tryptophan: A Precursor of Signaling Molecules in Higher Plants*; Springer, 2021; pp 273–289.

(65) Schenck, C. A.; Maeda, H. A. Tyrosine biosynthesis, metabolism, and catabolism in plants. *Phytochemistry* **2018**, *149*, 82–102.

(66) Etesami, H.; Glick, B. R. Bacterial indole-3-acetic acid: A key regulator for plant growth, plant-microbe interactions, and agricultural adaptive resilience. *Microbiol. Res.* **2024**, *281*, No. 127602.

(67) Aziz, R. A.; Ramesh, P.; Suchithra, K. V.; Stothard, P.; Narayana, V. K.; Raghu, S. V.; Shen, F.-T.; Young, C.-C.; Prasad, T. S. K.; Hameed, A. Comprehensive insights into the impact of bacterial indole-3-acetic acid on sensory preferences in *Drosophila melanogaster*. *Sci. Rep.* **2024**, *14* (1), No. 8311.

(68) Ahmed, V.; Verma, M. K.; Gupta, S.; Mandhan, V.; Chauhan, N. S. Metagenomic profiling of soil microbes to mine salt stress tolerance genes. *Front. Microbiol.* **2018**, *9*, No. 159, DOI: 10.3389/fmicb.2018.00159.

(69) Ferreira, C. M. H.; Soares, H. M. V. M.; Soares, E. V. Promising bacterial genera for agricultural practices: An insight on plant growth-promoting properties and microbial safety aspects. *Sci. Total Environ.* **2019**, *682*, 779–799.

(70) Mishra, P.; Mishra, J.; Arora, N. K. Plant growth promoting bacteria for combating salinity stress in plants – Recent developments and prospects: A review. *Microbiol. Res.* **2021**, *252*, No. 126861.

(71) Khan, M. A.; Sahile, A. A.; Jan, R.; Asaf, S.; Hamayun, M.; Imran, M.; Adhikari, A.; Kang, S.-M.; Kim, K.-M.; Lee, I.-J. Halotolerant bacteria mitigate the effects of salinity stress on soybean growth by regulating secondary metabolites and molecular responses. *BMC Plant Biol.* **2021**, *21* (1), 176.

(72) Safdarian, M.; Askari, H.; Shariati, V.; Nematzadeh, G. Transcriptional responses of wheat roots inoculated with *Arthrobacter nitroguajacolicus* to salt stress. *Sci. Rep.* **2019**, *9* (1), No. 1792.

(73) Zhang, G.; Bai, J.; Zhai, Y.; Jia, J.; Zhao, Q.; Wang, W.; Hu, X. Microbial diversity and functions in saline soils: A review from a biogeochemical perspective. *J. Adv. Res.* **2024**, *59*, 129–140.

(74) Khan, A.; Sirajuddin; Zhao, X. Q.; Javed, M. T.; Khan, K. S.; Bano, A.; Shen, R. F.; Masood, S. *Bacillus pumilus* enhances tolerance in rice (*Oryza sativa* L.) to combined stresses of NaCl and high boron due to limited uptake of Na<sup>+</sup>. *Environ. Exp. Bot.* **2016**, *124*, 120–129.

(75) Dong, Y.; Chen, R.; Graham, E. B.; Yu, B.; Bao, Y.; Li, X.; You, X.; Feng, Y. Eco-evolutionary strategies for relieving carbon limitation under salt stress differ across microbial clades. *Nat. Commun.* **2024**, *15* (1), No. 6013.

(76) Ha-Tran, D. M.; Nguyen, T. T.; Hung, S.-H.; Huang, E.; Huang, C.-C. Roles of Plant Growth-Promoting Rhizobacteria (PGPR) in Stimulating Salinity Stress Defense in Plants: A Review. *Int. J. Mol. Sci.* **2021**, *22* (6), No. 3154, DOI: 10.3390/ijms22063154.

(77) Wen, Z.; White, P. J.; Shen, J.; Lambers, H. Linking root exudation to belowground economic traits for resource acquisition. *New Phytol.* **2022**, *233* (4), 1620–1635.

(78) Kuypers, M. M. M.; Marchant, H. K.; Kartal, B. The microbial nitrogen-cycling network. *Nat. Rev. Microbiol.* **2018**, *16* (5), 263–276.

(79) Sah, S.; Krishnani, S.; Singh, R. *Pseudomonas* mediated nutritional and growth promotional activities for sustainable food security. *Curr. Res. Microb. Sci.* **2021**, *2*, No. 100084.

(80) Lyu, C.; Li, X.; Yu, H.; Song, Y.; Gao, H.; Yuan, P. Insight into the microbial nitrogen cycle in riparian soils in an agricultural region. *Environ. Res.* **2023**, *231*, No. 116100.

(81) Taha, R. S.; Seleiman, M. F.; Alotaibi, M.; Alhammad, B. A.; Rady, M. M.; Mahdi, A. H. A. Exogenous potassium treatments elevate salt tolerance and performances of *Glycine max* L. by boosting antioxidant defense system under actual saline field conditions. *Agronomy* **2020**, *10* (11), No. 1741.

(82) Jiang, J.; Wang, Y.-P.; Yang, Y.; Yu, M.; Wang, C.; Yan, J. Interactive effects of nitrogen and phosphorus additions on plant growth vary with ecosystem type. *Plant Soil* **2019**, *440* (1), 523–537.

(83) Zhang, C.; Lu, X.; Yan, H.; Gong, M.; Wang, W.; Chen, B.; Ma, S.; Li, S. Nitrogen application improves salt tolerance of grape seedlings via regulating hormone metabolism. *Physiol. Plant.* **2023**, *175* (2), No. e13896.

(84) Alrushaid, S.; Davies, N. M.; Martinez, S. E.; Sayre, C. L. Pharmacological characterization of liquiritigenin, a chiral flavonoid in licorice. *Res. Pharm. Sci.* **2016**, *11* (5), 355–365, DOI: 10.4103/1735-5362.192484.

(85) Van de Poel, B. Ethylene's fraternal twin steals the spotlight. *Nat. Plants* **2020**, *6* (11), 1309–1310.

(86) Wen, T.; Yu, G.; Hong, W.; Yuan, J.; Niu, G.-Q.; Xie, P.-H.; Sun, F.-S.; Guo, L.-D.; Kuzyakov, Y.; Shen, Q.-R. Root exudate chemistry affects soil carbon mobilization via microbial community reassembly. *Fundam. Res.* **2022**, *2* (5), 697–707.

(87) Baker, N. R.; Zhalnina, K.; Yuan, M.; Herman, D.; Ceja-Navarro, J. A.; Sasse, J.; Jordan, J. S.; Bowen, B. P.; Wu, L.; Fossum, C.; Chew, A.; Fu, Y.; Saha, M.; Zhou, J.; Pett-Ridge, J.; Northen, T. R.; Firestone, M. K. Nutrient and moisture limitations reveal keystone metabolites linking rhizosphere metabolomes and microbiomes. *Proc. Natl. Acad. Sci. U.S.A.* **2024**, *121* (32), No. e2303439121.

(88) Zhalnina, K.; Louie, K. B.; Hao, Z.; Mansoori, N.; da Rocha, U. N.; Shi, S.; Cho, H.; Karaoz, U.; Loqué, D.; Bowen, B. P.; Firestone, M. K.; Northen, T. R.; Brodie, E. L. Dynamic root exudate chemistry and microbial substrate preferences drive patterns in rhizosphere microbial community assembly. *Nat. Microbiol.* **2018**, *3* (4), 470–480.



CAS BIOFINDER DISCOVERY PLATFORM™

**PRECISION DATA  
FOR FASTER  
DRUG  
DISCOVERY**

CAS BioFinder helps you identify  
targets, biomarkers, and pathways

**Unlock insights**

CAS  
A division of the  
American Chemical Society